COBE-PREPRINT-NO-93-10A

C93/07/11.2

Fermilab Library 0 1160 0020713 8

12

COBE-Preprint-No-93-10A

The Cosmic Background Explorer (COBE) mission

John C. Mather

NASA Goddard Space Flight Center, Code 685
Laboratory for Astronomy and Solar Physics, Greenbelt, MD 20771

ABSTRACT

The Cosmic Background Explorer (COBE) satellite carries three instruments to measure the diffuse infrared and microwave background radiation from the early universe, along with more recent diffuse sources. It was developed by NASA's Goddard Space Flight Center and launched by a Delta rocket on November 18, 1989. It has produced the first measurements of structure in the Big Bang and has shown that the primeval heat radiation has a blackbody spectrum to extraordinary accuracy. The three instruments include a Far Infrared Absolute Spectrophotometer (FIRAS) to cover the range from 100 μm to 1 cm wavelength with a 7° resolution, a Diffuse Infrared Background Experiment (DIRBE) to map the sky from 1 to 300 μm with a 0.7° resolution in 10 broad bands, and a Differential Microwave Radiometer (DMR) to map the sky at 31.5, 53, and 90 GHz with a 7° resolution. The designs of the instruments and spacecraft are described, and the primary results are summarized.

1. INTRODUCTION AND MISSION OBJECTIVES

Since the discovery of the cosmic microwave background radiation (CMB) by Penzias and Wilson in 1964[1], numerous experiments have been done to measure its properties. These are difficult because the radiation is faint and is absorbed by the terrestrial atmosphere, and because emission from our own Galaxy adds significantly at wavelengths longer than 1 cm or shorter than 0.7 mm. The CMB has peak intensity at millimeter wavelengths, corresponding to its temperature of about 3 K. According to the Big Bang theory, this radiation is the remnant of the primeval explosion that propelled the expansion of the entire universe about 15 billion years ago. It is the primary radiative relic of the Big Bang, and it is vitally important to measure its intensity as a function of frequency, angle, polarization, and coherence state.

After the universe expanded sufficiently to cool and allow gravity to pull together matter into objects, the familiar catalog of astronomical objects was formed. These include stars with their planets, grouped into galaxies, which are themselves grouped into clusters and superclusters with enormous empty regions 300 million light years across between them. This process is not understood at all, although there are an abundance of theories. We can look back in time by looking far away, but distant objects are very faint and difficult to study. On the other hand, the accumulated radiation from energy liberated in the formation of stars and galaxies must fill the universe and should be observable as a diffuse infrared background radiation. It is expected to occupy the infrared spectral band because it the expansion of the universe redshifts the radiation from its original visible or ultraviolet wavelengths.

The COBE was designed to measure both of these background radiation fields in ways that are not possible without a space environment. The terrestrial atmosphere blocks much of the desired spectral band, and would condense on the cooled instruments necessary to observe the radiation. Long observing times are also needed to build up signal-to-noise ratio for the very faint background radiation, given the sensitivities of detectors. The space environment also permits accurate calibration and careful tests for systematic errors in the instruments.

The primary scientific objectives are to measure the spectrum of the CMB to test the Big Bang theory, to measure the anisotropy of the CMB to search for the primeval seeds that would lead to the formation of galaxies and clusters of galaxies, and to detect the cosmic infrared background energy liberated by the first generation of stars and galaxies. Secondary objectives include measurements of the diffuse light from interstellar and interplanetary dust, the general distribution of starlight in the Galaxy, the measurement of far infrared radiation from interstellar molecules, atoms, and ions, and the determination of polarization of the background radiation at wavelengths of 1 to 3.5 μm .

The detailed requirements of the mission follow from the general specification that the accuracy of the cosmological measurements be limited only by our astrophysical environment. This implies that sensitivities should be sufficient to produce a high signal to noise ratio on the Galactic and interplanetary sources of diffuse radiation, and that the calibration and systematic error sources should be small by comparison. This level of sensitivity and accuracy

permits detailed modeling of the local astrophysical environment so that its effects may be subtracted from the total, yielding definitive cosmological results that are close the best that can be achieved from this location in the universe.

Numerous papers giving overviews, implications, and additional detailed information about *COBE* have been presented[2-16].

2. MISSION CONCEPT - ORBIT, ATTITUDE, SPACECRAFT

The COBE has three instruments to span the wavelength range from 1 μm to 1 cm with overlapping wavelength ranges. The three instruments include a Far Infrared Absolute Spectrophotometer (FIRAS) to cover the range from 100 μm to 1 cm wavelength with a 7° resolution, a Diffuse Infrared Background Experiment (DIRBE) to map the sky from 1 to 300 μm with a 0.7° resolution in 10 broad bands, and a Differential Microwave Radiometer (DMR) to map the sky at 31.5, 53, and 90 GHz with a 7° resolution.

The two infrared instruments operate in vacuum and are cooled by liquid helium at 1.4 K. The helium lasted for 10 months and the cryostat interior then warmed up to approximately 60 K. The microwave radiometers are mounted on the circumference of the cryostat and do not require cryogen, and are still in operation. The cryostat and radiometers are protected by a conical shield, deployed after launch, which prevents the Earth and Sun from illuminating the instruments. The shield aperture is coplanar with the apertures of the cryostat and instruments, so that there is no direct geometrical optics path for the shield to heat the instruments or radiate into their apertures. The spacecraft and instruments are shown schematically in Fig. 1.

2.1 Orbit

The orbit is circular at 900 km altitude, with an inclination to the equator of 99° and an ascending node at 6 PM. This is sun-synchronous, meaning that the gravitational field of the Earth makes the orbit precess at 1 rotation per year to follow the apparent motion of the Sun. The orbit plane is approximately perpendicular to the line to the Sun, so that the instruments can always look away from the Earth and perpendicular to the Sun. This geometry is unique among orbit choices and permits excellent protection of the instruments. The choice of altitude is governed by a compromise between the effects of the residual atmosphere, which could condense on the helium-cooled surfaces and might emit infrared radiation when excited by the passage of the satellite, and the effects of the trapped particle radiation in the Van Allen belts. The orbit period is 103 minutes, giving 14.0 orbits/day. The orbit is shown in Fig. 2. The COBE was launched at dawn into this orbit by Delta rocket number 189 at 1434 UT on November 18, 1989 from Vandenberg Air Force Base in California.

One serious effect of this altitude choice is that the COBE passes into the Earth's shadow for a portion of each orbit up to 20 minutes long for about 2 months of each year, centered around the June solstice. Consequently, the power system must include batteries, the solar cell array must be larger, and the attitude control system must be capable of operating without a solar reference. Circular sunsynchronous orbits with altitude greater than about 1400 km do not suffer from this effect, but would have exposed the COBE to more particle radiation and would have required a larger rocket or smaller satellite.

2.2 Attitude

The spacecraft is oriented with its symmetry axis approximately perpendicular to the Sun line, and is capable of set points ranging from 90° to 98° away. The nominal angle was 94° for most of the mission, and tests were done to search for effects of the Sun by tilting as close as 91.5° and as far away as 98° . The symmetry axis is also maintained approximately vertical and perpendicular to the orbit velocity vector, but tipped back by about 6° to reduce the incident flux of residual atmospheric oxygen and hydrogen atoms striking the instrument apertures. No effect of the residual atmosphere on the instruments has been detected. The actual angle between the axis and the velocity vector varies by several degrees from the average of 96° as a result of the complex interactions of the attitude control system and the fact that the vertical direction is not in general equivalent to 94° away from the Sun.

A minor effect of this systematic tilt away from the vertical is that the thrust vector of the escaping helium, which

is directed along the spin axis by a nozzle on the bottom of the spacecraft, has a component along the orbit velocity vector. As a result, the orbit altitude gradually decayed at a rate of about 30 m/day, much larger than that due to atmospheric drag, and in a somewhat irregular way. This caused some difficulty with planning the exact times to command the satellite more than 2 weeks in advance.

The spacecraft spins about its symmetry axis at 0.8 rpm to scan the lines of sight for the DMR and DIRBE rapidly. Both instruments receive light from angles 30° from the spin axis. As the spacecraft spins and orbits, the lines of sight trace out a cycloidal path on the sky that covers a band 60° wide. The line of sight of the FIRAS is along the spin axis. As the orbit plane precesses at the rate of one rotation per year, the instruments sweep out the whole sky in 6 months. These lines of sight are illustrated in Fig. 3.

At the same season that the COBE passes through the Earth's shadow, it also passes between the Earth and the Sun for an equal amount of time half an orbit later. This means that there is no orientation for the spacecraft in which the Earth and Sun can simultaneously be kept from illuminating the aperture plane of the instruments and shield. The orbit plane varies as much as 32.5° from the Sun line, but the Earth horizon is depressed by only 28° . Allowing for the tilt of the spacecraft away from the Sun, the Earth limb rose as high as 9° above the plane of the shield. Data taken during this period by the FIRAS and DMR instruments were not as accurate as those taken at other seasons, but the DIRBE photometric quality was not affected by the heat from the Earth.

The attitude control system of the spacecraft uses Sun and Earth limb sensors for long term control, and rate integrating gyros for short term feedback and precise interpolation. Control torques are applied to momentum wheels and magnetic torquer bars acting on the Earth's magnetic field. The spin of the spacecraft about the symmetry axis is driven by two large momentum wheels, whose angular momentum is equal and opposite to that of the spacecraft body, giving a total spin momentum of zero. Since there is no net spin momentum, the spacecraft does not act like a gyro itself, and only small control torques are needed to move its spin axis to follow the vertical direction.

The small control torques needed are provided by a highly redundant control system. There are three small inertia wheels with their axes oriented 120° apart and perpendicular to the spacecraft spin axis. An angular momentum component perpendicular to the spacecraft spin axis can be stored by a linear combination of the spins of any two of these three small wheels, so that one may fail without jeopardizing the system. Each wheel is controlled by a redundant set of servos and sensors, and cross-strapping is provided so that a failed sensor can be replaced by a linear combination of the sensors for the other two wheels. Tests in orbit and computer simulations have shown that the system works very well even if one servo is disabled, and simulations suggest that it will still work with less accuracy even if two are disabled. This is fortunate, since only 4 days into the mission one of the gyros failed, and another one became erratic 1.5 years later. No scientific data were lost and the spacecraft never allowed the Sun to illuminate the instruments.

In data reduction on the ground, coarse attitude parameters are calculated by using telemetered data from the attitude control sensors. The Sun and Earth directions are measured in spacecraft body coordinates and are transformed to inertial coordinates using the spacecraft ephemeris. These are then used to compute quaternions and rotation matrices describing the spacecraft orientation. The data are smoothed and interpolated using the gyro signals to produce attitude solutions good to 4 arcmin (1 σ), adequate to meet the initial requirements for the FIRAS and DMR. The DIRBE with its smaller beam size (0.7° rather than 7°) requires a more accurate attitude solution. This fine aspect is determined by using gyro data to interpolate between the positions of known stars detected in the short wavelength bands of the DIRBE instrument. The fine aspect solution has an accuracy of 1.5 arc min (1 σ) and is now used in the analysis of data from all three instruments.

2.3 Power

The spacecraft is powered by three double sided solar array wings, deployed immediately after launch. They provide a peak capacity of 1280 W at launch and an average capacity of 750 W at the end of the first year. The nominal spacecraft and instrument power consumption is 542 W, and the extra capacity is required to charge the batteries for the passages through the Earth's shadow. The power generated by the arrays varied sinusoidally with a 7% peak to peak amplitude as a result of the eccentricity of the Earth's orbit. It also declined by about 3% by the end of the first year because of UV and cosmic ray damage. A noticeable and unanticipated increase occurred when the COBE

flew over the Antarctic ice cap, and almost exceeded the capacity of the power regulators.

The power generated by the arrays is coupled directly to the spacecraft power bus at 28 volts. Regulation is provided by controlled shunts which dissipate the extra power as heat and radiate it away on the bottom of the spacecraft. When the satellite passes into the shadow the control system automatically draws power from the battery and steps up the voltage to the required 28 volt level.

The power control circuitry was designed and tested extensively to reduce the interference to negligible levels. Low noise converters used separate grounds, multiple shields, and nested subregulators for critical components. A high degree of redundancy was provided but no failures occurred.

2.4 Communications

The COBE uses Motorola S-band transponders to transmit and receive data and commands. Two antennas are provided on a mast on the bottom of the spacecraft, one for direct communications with the ground station at Wallops Flight Facility in Virginia, and one for relay through the Tracking and Data Relay Satellite System (TDRSS). The TDRSS is used in the multiple access mode approximately every other orbit, 7 times a day, to monitor the satellite and send commands. The single access mode was available as a backup for the primary data recovery channel as well, but was never needed. Data received by the TDRSS are relayed to a ground terminal at White Sands, NM, and relayed again by satellite to Goddard Space Flight Center. The ground system at Wallops is used to receive the accumulated data from each day of operations, with a total of 4 or 5 opportunities per day.

Data are recorded on two RCA tape recorders and played back at 160 times the real time rate, allowing 24 hours of data to be transmitted in 9 minutes. The data are stored in time division multiplexed format, with 1716 bits/second allocated to DIRBE, 1362 to FIRAS, 250 to DMR, and 768 to the spacecraft, for a total of 4096.

Commands are stored in a traditional system built by Gulton Industries. They are stored in a memory capable of holding 4096 commands, executed over a 48 hour period, with limited subroutine capability. Management of this memory proved difficult because there were more commands necessary per day than anticipated.

2.5 Spacecraft Structure

The original 1974 proposal for the COBE called for a launch on a Delta expendable rocket. However, during the design phase NASA adopted the Shuttle as the universal launch vehicle. The Shuttle was capable of a large payload, so no deployable parts were required, but it could not reach the required COBE altitude and a hydrazine propulsion system was needed. After the Challenger explosion, NASA terminated the development of launch facilities for Shuttles at the Vandenberg Air Force Base. A west coast launch is required to achieve the COBE polar orbit inclination.

The COBE was therefore redesigned, after the instruments and electronic systems had been constructed. Approval for the redesigned COBE was granted in late 1986, and it was launched three years later. No large changes were needed to the instruments or the existing electronics, and the spacecraft weight was cut in half. The hydrazine propulsion system was no longer needed, and the mechanical structure was much smaller and lighter than before. The battery was made smaller to save weight, and minor redesign was necessary for the power supply electronics, the attitude control electronics, the torquer bars, and the main electrical harness. The electronically steerable antenna was replaced by an omni antenna, and both antennas were mounted on a deployable boom. The solar cell panels, which had been mounted on the body of Shuttle version of the COBE, were redesigned as a set of three folding wings. The sunshield was completely redesigned. The DMR radiometers were repackaged using the same microwave hardware, and were attached directly to the cryostat to save weight and space. The vibration loads for the Delta were different from those on the Shuttle, requiring a modification to the tuning fork chopper for the DIRBE. The final COBE had a mass of 2270 kg, a length of 5.49 m, a diameter of 2.44 m with solar panels and shield folded for launch, and a diameter of 8.53 m with panels deployed.

2.6 Cryostat

The cryostat is a 650 liter superfluid helium cryostat which uses a porous plug to separate the liquid and gas phase.

It is similar to the cryostat used by the IRAS mission[17] and was built by Ball Aerospace Division. An aperture cover protected the instruments during ground operations and was ejected in orbit after 3 days of outgasing. The cover included no cryogenics of its own but did have a protective shield for the DIRBE primary mirror. The helium temperature was approximately 1.4 K throughout the mission, and was very stable except when electrical power dissipation in the FIRAS and DIRBE instruments was changed during the calibrations. The detectors and optics were warmer than the helium, from 1.5 to 1.6 K.

The helium lasted for 10 months of orbital operations. The helium loss rate was governed by the instrument power dissipation, by parasitic heat inputs, and by radiation from the Earth limb during the summer season. The outer shell of the cryostat was painted white for low optical absorptivity and high infrared emissivity. The temperature of the outer shell of the cryostat was approximately 130 K as planned. Following the exhaustion of the helium, the interior of the cryostat warmed up to about 60 K over the course of several months.

The FIRAS and DIRBE instruments were installed together in a Cryogenic Optical Assembly, which was provided with 5 120 pin blind mate connectors and a blind mate fiber optic connector. The entire assembly was lowered into the cryostat and bolts were tightened to attach it to a matching flange in the cryostat. This flange served to conduct all the heat from the instruments to the liquid helium. Thermal impedances raised the instrument temperature approximately 0.1 to 0.2 K above the helium temperature.

2.7 Sun-Earth Shield

The protective conical shield around the cryostat and instruments was made from 12 honeycomb panels, covered with multilayer insulation blankets. The 12 panels were hinged at the bottom end and pivoted out after launch, and the triangular gores between them were spanned by flexible multilayer insulation blankets that were folded for launch. The outer layers facing the Sun were aluminized Kapton, with the aluminum behind the Kapton, to give a high reflectivity and a high infrared emissivity. The internal temperature of the shield in orbit was approximately 180 K. The shield also included hinged dust covers for the DMR radiometers, which were pulled away from the instruments when the shield was deployed.

2.8 Test Program

The COBE was tested extensively prior to launch. Electronic parts were screened, and very large numbers failed. Subassemblies were tested individually and at higher levels of integration. A second mechanical model of the spacecraft was built for mechanical tests, and the whole COBE was vibrated on a 35,000 lb force shaker with sinusoidal and random loads. Particular attention was given to "pogo" modes of the launch vehicle, which were expected to produce several g's of acceleration at 17 and 32 Hz. The latter frequency was close to a primary resonance of the helium cryostat and to the resonance of a tuning fork chopper in the DIRBE.

The spacecraft was also tested in a thermal vacuum chamber with everything installed except solar cells and sunshield. Tests revealed a mysterious and fortunately unrepeated failure in the DIRBE microprocessor. They also showed a problem in the control electronics for the moving mirror in the FIRAS, which was repaired before launch. Mechanical tests also showed that the moving calibrator for the FIRAS instrument would not have stayed in position in flight. This was a result of an electrical cable which became unexpectedly stiff at low temperatures. This was also repaired before flight, without removing the instruments from the cryostat.

Another significant discovery in the test program was that the Earth sensors were also sensitive to pulsed RF radiation at the levels predicted from the NORAD radars. To protect these sensors, Faraday cages were made of thin wire screen. RF tests also showed some pickup by the infrared detectors, but the orbital environment was much quieter and no RF problems appeared in flight. The spacecraft transmitter, which is FM modulated, had no effect on the instruments.

Numerous technical papers have been published about the COBE. Papers that are not specific to the instruments are listed here. Contamination control was described by Barney[18], and test facilities for thermal balance tests by Milam[19]. The dewar was described by Hopkins and Castles[20], its thermal performance was discussed by Hopkins and Payne[21], Volz and Ryschkewitsch[22], Volz *et al.* [23], Volz *et al.* [24], and Volz and DiPirro[25]. The thermal design of

the cryogenic instruments was given by Mosier *et al.* [26], and cryogenic tests were discussed by Coladonato *et al.* [27]. Optical alignments were described by Sampler[28], and attitude control was discussed by Bromberg and Croft[29].

3. INSTRUMENTS AND RESULTS

3.1 DMR description

The DMR is a set of 6 differential microwave radiometers, using Schottky diode mixers, HEMT IF amplifiers, and ferrite Dicke switches, and is described by Smoot *et al.* [30]. It uses circular corrugated horn antennas to define 7° beams on the sky, 60° apart. As the spacecraft spins, it interchanges the beams rapidly to determine the instrument baseline signal and separate the part of the signal due to the sky. Over the course of half a year, all possible combinations of pixels 60° apart are compared.

The DMR radiometers are designed to search for anisotropies (differences in brightness) of the CMBR with a mean sensitivity better than 0.15 mK rms (at frequencies of 53 and 90 GHz), and 0.3 mK (at 31.5 GHz), per 7° pixel on the sky after one year of observation. The 31.5 GHz radiometers are operated at 300 K, and those at higher frequencies are radiatively cooled to 140 K. The multiple frequencies were selected to bracket the region where galactic synchrotron emission, free-free emission, and radiation by interstellar dust are least, and to distinguish these sources from the CMB. Gain calibrations are obtained from the Moon, from internal secondary reference noise sources, and from the modulation of the CMB dipole by the Earth's motion around the Sun (Bennett *et al.*[31]).

In the data analysis for each radiometer channel, a baseline is subtracted and the data are calibrated. Data are rejected when the limb of the Earth is higher than 1° below the Sun/Earth shield plane, when the Moon is within 25° of a beam center, when any datum deviates from the daily mean by more than 5σ, or when the spacecraft telemetry or attitude solution is of poor quality. Small corrections are applied to remove the estimated emission from the Moon and Jupiter in the remaining data. Corrections are also applied to remove the Doppler effects from the spacecraft's velocity about the Earth and the Earth's velocity about the solar system barycenter. A least-squares minimization is used to fit the data to spherical harmonic expansions and to make sky maps with 6144 nearly equal area pixels using a sparse matrix technique[5,32]. The DMR instrument is sensitive to external magnetic fields. Extra equations are included in the sparse matrix to allow these magnetic susceptibilities to be fit separately as a linear function of the Earth's field and the radiometer orientation. The magnetic corrections are on the scale of 10 to 100 μK in the time-ordered data. Residual uncertainties in the individual radiometer channel maps, after correction, are typically 2 μK and never more than 8.5 μK.

3.2 DMR Results

The primary DMR result is the detection of the primeval density fluctuations thought to be the origin of the large scale structure of the universe. Observationally these are seen as fluctuations in brightness of the cosmic background radiation, with characteristic sizes of the order of 15° and amplitude of 30 μK, approximately 11 parts per million of the total brightness. According to the Big Bang theory, these brightness fluctuations arise from differential gravitational redshifts of the photons, as they climb out of different gravitational potentials in the early universe. This phenomenon is called the Sachs-Wolfe effect. The darker regions are thus denser. They are seen as they were at a time about 300,000 years after the Big Bang, when the photons were last scattered by free electrons. After that time, the primordial plasma became neutral atomic gas and thus transparent.

These gravitational potentials are thought to be the primeval seeds that produce the gravity that pulls material into large clusters and superclusters of galaxies. Present day structures as large as hundreds of millions of light years have now been measured with ground based telescopes. The structures measured by the DMR are now much larger, stretching across the whole sky even when the universe was 1000 times smaller than it is now.

The amount of fluctuation of temperature is a function of the angular size. The DMR observations confirm the predictions of the inflationary theory of the Big Bang, which are that there should be no preferred physical scale. Instead, there should be a power law for the random fluctuations as a function of size, with a particular index which corresponds to equal amounts of gravitational potential fluctuation on all size scales. This is called the Peebles-Harrison-Zeldovitch spectrum.

Smoot et al.[33] presented preliminary DMR results based on six months of data. Smoot et al.[34] describe results based upon the first year of DMR data, Bennett et al.[31] describe the calibration procedures, Kogut et al.[35] discuss the treatment of systematic errors, and Bennett et al.[36] discuss the separation of cosmic and Galactic signals. Wright et al.[37] compare these data to other measurements and to models of structure formation through gravitational instability. Previously published large-angular-scale anisotropy measurements include Fixsen et al.[38], Lubin et al.[39], Klypin et al.[40], and Meyer et al.[41]. Some excellent reviews of CMB anisotropy and cosmological perturbation theory include references 42-47.

The DMR maps are dominated by the dipole anisotropy and the emission from the Galactic plane. The dipole anisotropy ($\Delta T/T \approx 10^{-3}$) is seen consistently in all channels with a thermodynamic temperature amplitude 3.36±0.1 mK in the direction $l = 264.7° \pm 0.8°$, $b = 48.2° \pm 0.5°$, consistent with the FIRAS results. Our motion with respect to the CMB (a blackbody radiation field) is assumed to produce the dipole anisotropy, so the dipole and associated $\approx 1.2\ \mu$K rms kinematic quadrupole are removed from the maps.

3.3 FIRAS Instrument

The FIRAS instrument is a polarizing Michelson interferometer (Mather[14]) with two separate spectral bands. The low frequency band, extending from 0.5 mm to 1 cm, was designed to obtain a precision comparison between the CMB spectrum and a Planckian calibration spectrum. The objective was to attain, in each 5% wide spectral element and each 7° pixel, an accuracy and sensitivity of $\nu I_\nu \cong 10^{-9}$ W m^{-2} sr^{-1} which is 0.1% of the peak brightness of a 2.7 K blackbody. The high frequency band, with a useful spectral range from 0.12 mm to 0.5 mm, was designed to measure the emission from dust and gas in our galaxy and to remove the effect of galactic radiation on the measurements of the CMB made in the low frequency band.

The instrument directly measures the difference between the sky signal in its 7° beam and that from a temperature-controlled internal reference body. The best apodized spectral resolution is 0.2 cm $^{-1}$ (6 GHz). The in-orbit absolute calibration of FIRAS was accomplished by inserting an external blackbody calibrator periodically into the mouth of the horn. The calibrator is a precision temperature-controlled blackbody, with an emissivity greater than 0.999. The FIRAS uses bolometric detectors in both bands. A more complete description of the FIRAS is in preparation for this conference[48].

An unanticipated problem with FIRAS occurred after launch. A position sensor in the mirror transport mechanism of the interferometer was triggered by energetic charged particles trapped in the magnetic field of the Earth, especially during passages through the South Atlantic Anomaly (SAA). As a result, the transport mechanism went to its end-of-travel and continued to drive against its stop, dissipating excess power into the dewar. Once understood, the problem was largely overcome by commanding the transport mechanism to cease scanning on entry to the SAA and to resume normal operation on leaving the SAA. This anomaly somewhat shortened the lifetime of the helium.

3.4 FIRAS Results

In 1993, Fixsen *et al.* [49] presented a new calibration model for the FIRAS. This model includes an estimated correction to the temperature scale of -4 mK, based on the self-consistency of the photometric calibration. This is essentially a determination of the color temperature scale from the wavelength scale and the Planck functional form. Based on this calibration, Mather *et al.* [50] used 6 weeks of interleaved sky and calibration data to determine the extragalactic background spectrum. They modeled the Galactic spectrum and fitted it by geometrical and spectral methods to remove it and find the mean cosmic background radiation spectrum. The mean temperature is 2.726 ± 0.010 K, over the frequency range from 2 to 20 cm^{-1}. Over this range the maximum deviation from the blackbody form is less than 0.03%, with a weighted rms value of only 0.01%. Fits to the dimensionless cosmic distortion parameters give 95% confidence limits of $|\mu/kT| < 3.3 \times 10^{-4}$ and $|y| < 2.5 \times 10^{-5}$ respectively.

The implications of these limits are summarized by Wright *et al.* [51]. Less than 0.03% of the energy in the CMB was added to it after the first year of the expansion. Less than 10^{-4} of the diffuse X-ray background can be produced by a smooth hot intergalactic medium. Less than 1% of the mass of hydrogen could be burned by Population III stars after a redshift of 80, and less than 1% of the hydrogen could be burned by an evolving population of galaxies like those seen by the IRAS. These limits are based on $\Omega_{baryon} = 0.0125h^2$. The Steady State theory is conclusively

ruled out, as are theories of a Cold Big Bang with needle-shaped dust to thermalize stellar radiation.

The dipole anisotropy of the CMB, presumed due to our peculiar motion relative to the Hubble flow, can be seen clearly in the FIRAS data, and is consistent with previous results[52]. Fixsen *et al.* [53] give the most recent dipole results. The FIRAS data show for the first time that the spectrum of the dipole is that expected from the Doppler shift acting on a blackbody spectrum. The dipole amplitude measured by FIRAS is 3.343 ± 0.016 mK in the direction $(\alpha, \delta) = (168.9° \pm 0.5°, -7.5° \pm 0.5°)$, (l,b)=$(265.6°, 48.3°)$. The color temperature of the dipole is 2.714 ± 0.014 K, and the maximum deviation of the dipole spectrum from the expected form is only 0.005% of the peak intensity of the CMB.

FIRAS results also include the first nearly all-sky, unbiased, far infrared survey of the galactic emission at wavelengths greater than 120 μm[54]. Wright et al.[54] present a map of the dust emission across the sky from the *COBE* FIRAS experiment. The total far infrared luminosity of the Galaxy is inferred to be $(1.8 \pm 0.6) \times 10^{10} L_{\odot}$.

Wright et al. report that spectral lines from interstellar [C I], [C II], [N II], and CO are detected in the mean galactic spectrum, $g(\nu)$. The lines of [C II] at 158 μm and [N II] at 205.3 μm were sufficiently strong to be mapped. This is the first observation of the 205.3 μm line. Wright et al. interpret the [C II] line as coming from photodissociation regions and the [N II] lines as partially arising from a diffuse warm ionized medium and partially arising from dense H II regions. Petuchowski & Bennett[55] further elaborate on this conclusion by apportioning the [C II] and [N II] transition line intensities among various morphologies of the interstellar medium. Petuchowski & Bennett (in preparation) have conducted observations on NASA's Kuiper Airborne Observatory to measure the scale height of the 205.3 μm [N II] line with a much higher angular resolution ($\sim$1 arcmin) than FIRAS.

3.5 DIRBE Description

The experimental approach is to obtain absolute brightness maps of the full sky in 10 photometric bands (J[1.2], K[2.3], L[3.4], and M[4.9]; the four IRAS bands at 12, 25, 60, and 100 μm; and 140 and 240 μm bands). To facilitate discrimination of the bright foreground contribution from interplanetary dust, linear polarization is also measured in the J, K, and L bands, and all celestial directions are observed hundreds of times at all accessible angles from the Sun in the range 64° to 124°. The instrument rms sensitivity per field of view in 10 months is $\lambda I(\lambda) = (1.0,\ 0.9,\ 0.6,\ 0.5,\ 0.3,\ 0.4,\ 0.4,\ 0.1,\ 11.0,\ 4.0) \times 10^{-9}$ W m^{-2} sr^{-1}, respectively for the ten wavelength bands listed above. These levels are generally well below both estimated CIB radiation contributions[56] and the total infrared sky brightness.

The DIRBE instrument is an absolute radiometer, utilizing an off-axis Gregorian telescope with a 19-cm diameter primary mirror. Since the DIRBE was designed to make an absolute measurement of the spectrum and angular distribution of the diffuse infrared background it must have extremely strong rejection of stray light. The optical configuration[57] has strong rejection of stray light from the Sun, Earth limb, Moon other off-axis celestial radiation, and parts of the *COBE* payload[58,59]. Stray light rejection features include both a secondary field stop and a Lyot stop, super-polished primary and secondary mirrors, a reflective forebaffle, extensive internal baffling, and a complete light-tight enclosure of the instrument within the *COBE* dewar. Additional protection is provided by the Sun and Earth shade surrounding the *COBE* dewar, which prevents direct illumination of the DIRBE aperture by these strong local sources. The DIRBE instrument, which was maintained at a temperature below 2 K within the dewar as long as helium was present, measures absolute brightness by chopping between the sky signal and a zero flux internal reference at 32 Hz using a tuning fork chopper. The synchronously demodulated signal is averaged for 0.125 second before transmission to the ground. Instrumental offsets are measured by closing a cold shutter located at the prime focus. All spectral bands view the same instantaneous field-of-view, 0.7° x 0.7°, oriented at 30° from the spacecraft spin axis. This allows the DIRBE to modulate the angle from the Sun by 60° during each rotation, and to sample fully 50% of the celestial sphere each day. Four highly-reproducible internal radiative reference sources can be used to stimulate all detectors when the shutter is closed to monitor the stability and linearity of the instrument response. The highly redundant sky sampling and frequent response checks provide precise photometric closure over the sky for the duration of the mission. Calibration of the photometric scale is obtained from observations of isolated bright celestial sources. Careful measurements of the beam shape in pre-flight system testing and during the mission using scans across bright point sources allow conversion of point-source calibrations to surface brightness calibrations.

The data obtained during the helium temperature phase of the mission are of excellent photometric quality, showing good sensitivity, stability, linearity, and stray light immunity. Few artifacts are apparent other than those induced by energetic particles in the South Atlantic Anomaly and variations in instrument temperature. Both of these effects will be removed in final data processing. Strong rejection of off-axis radiation sources is confirmed by the absence of response to the Moon (which saturates the response in all detectors when in the field of view) until it comes within about 3° of the field of view. The sensitivity per field of view, listed above, is based on noise measured with the shutter closed and response determined from measurements of known celestial sources. The noise when the shutter was open is somewhat above the shutter-closed values due to discrete source confusion. The nuclear radiation environment in orbit caused very little response change (<1%) in all detectors except the Ge:Ga photoconductors used at 60 and 100 μm. Thermal and radiative annealing procedures applied to these detectors following passages through the South Atlantic Anomaly allow response correction to about 1% at these wavelengths. It is expected that fully reduced DIRBE sky maps will have photometric consistency over the sky better than 2% at each wavelength, nearest neighbor band-to-band (color) brightness accuracy of 3% or better, and absolute intensity scale accuracy better than 20%. Due to strongly non-linear response of the Ge:Ga detectors, the 60 and 100 μm data may not meet these goals.

3.6 DIRBE Results

Preliminary results of the DIRBE experiment have been described previously[8,9,60–66]. Qualitatively, the initial DIRBE sky maps show the expected character of the infrared sky. For example, at 1.2 μm stellar emission from the galactic plane and from isolated high latitude stars is prominent. Zodiacal scattered light from interplanetary dust is also prominent. These two components continue to dominate out to 3.4 μm, though both become fainter as wavelength increases. Because extinction at near infrared wavelengths is far less than in visible light, the disk and bulge stellar populations of the Milky Way are dramatically apparent at these wavelengths. At 12 and 25 μm, emission from the interplanetary dust dominates the sky brightness. As with the scattered zodiacal light, the sky brightness is strongly dependent upon ecliptic latitude and solar elongation angle. At wavelengths of 60 μm and longer, emission from the interstellar medium dominates the galactic brightness, and the interplanetary dust emission becomes progressively less apparent. The patchy infrared cirrus noted in IRAS data[67] is evident at all wavelengths longer than 25 μm. False color all sky images prepared from DIRBE data have recently been presented by Hauser[61].

Initial galactic studies based on DIRBE data have recently been reported. These include investigation of the warp of the plane in the stellar and interstellar dust components[63], examination of the color and extinction of integrated galactic starlight[64], study of asymmetries in the starlight from the bulge, supporting the suggestion of a stellar bar[65], and study of physical conditions in the interstellar medium in the galactic plane[66]. The first results of polarization measurements with the DIRBE have also been presented[62].

In searching for the extragalactic infrared background, the most favorable conditions are directions and wavelengths of least foreground brightness. In general, because of the strong interplanetary dust foreground and the relatively modest gradient of that foreground over the sky, the infrared sky is faintest at high ecliptic latitude. A preliminary DIRBE spectrum of the sky brightness toward the south ecliptic pole was presented by Hauser et al.[60]. The strong foreground from starlight and scattered sunlight at the shortest wavelengths, a relative minimum at 3.4 μm, emission dominated by interplanetary dust peaking around 12 μm, and generally falling brightness from there out to submillimeter wavelengths. The most likely wavelengths for detecting extragalactic backgrounds are near the 3.4 μm window and in the submillimeter range.

4. DATA PRODUCTS AND PLANS

Extensive data products from the *COBE* mission consisting of calibrated maps and spectra with associated documentation will be made publicly available. The *COBE* databases have been described by White & Mather[68]. The design of the *COBE* software system has been described by Cheng[69]. All *COBE* data processing and software development for analysis take place at the Cosmology Data Analysis Center (CDAC) in Greenbelt, MD, a facility developed by the *COBE* project for that purpose. This facility, and the software tools developed there, will become available to the scientific community when the data products become public. The initial data products are planned for release in mid 1993, and will be calibrated and corrected for almost all known instrumental and spacecraft effects. The initial maps will include all 10 DIRBE bands and the high frequency FIRAS band for the galactic plane, including

the nuclear bulge. The DMR data will be all-sky maps from the first year of data for all six radiometers. Full sky maps from all three *COBE* instruments, spanning four decades of wavelength, are planned for release in mid-1994. After proper characterization, calibration and the removal of sources of systematic error have been accomplished, the data gathered by *COBE*'s three instruments will constitute a comprehensive data set unprecedented in scope and sensitivity for studies of cosmology, galactic astronomy, and solar system science.

5. ACKNOWLEDGEMENTS

The National Aeronautics and Space Administration/Goddard Space Flight Center (NASA/GSFC) is responsible for the design, development, and operation of the Cosmic Background Explorer (COBE), under the scientific guidance of the COBE Science Working Group. GSFC is also responsible for the software development and the final processing of the mission data. In addition to the authors of this paper, many people have made essential contributions to the success of *COBE* in all its stages, from conception and approval through hardware and software development, launch, and flight operations. To all these people, in government agencies, universities, and industry, the authors extend their thanks and gratitude. In particular, we thank the large number of people at the GSFC who brought this challenging in-house project to fruition.

6. REFERENCES

1. Penzias, A. A., & Wilson, R. W., *ApJ*, 142, 419, 1965.
2. Mather, J. C. et al., *IAU Colloq. 123, Observatories in Earth Orbit and Beyond, Proc.*, ed. Y. Kondo, 9, Kluwer, Boston, 1990.
3. Mather, J. C. et al., *AIP Conf. Proc. After the First Three Minutes*, 222, 43, ed. S. S. Holt, C L. Bennett, & V. Trimble, AIP, New York, 1991.
4. Mather, J. C., *Highlights Astron.*, 1991, in press.
5. Janssen, M. A. & Gulkis, S., *Proc. The Infrared and Submillimetre Sky After COBE, Les Houches*, 391, ed. M. Signore & C. Dupraz, Kluwer, Dordrecht, 1991.
6. Wright, E. L. *Ann. NY Acad. Sci., Proc. Texas-ESO-CERN Sym*, 647, 190, 1990.
7. Wright, E. L,*Proc. The Infrared and Submillimetre Sky After COBE, Les Houches*, 231, ed M. Signore & C. Dupraz, Kluwer, Dordrecht, 231, 1991.
8. Hauser, M. G., *Proc. Conf. Infrared Astronomy and ISO, Les Houches*, 1991 June in press.
9. Hauser, M. G. *Highlights Astron.*, in press, 1991.
10. Smoot, G. F. et al., *AIP Conf. Proc., After the First Three Minutes*, 222, 95, ed. S. S. Holt, C. L. Bennett, & V. Trimble, AIP, New York, 95, 1991.
11. Smoot, G. F. *Highlights Astron*, in press, 1991.
12. Bennett, C. L. *Highlights Astron*, in press, 1991.
13. Boggess, N. W. *Highlights Astron*, in press, 1991.
14. Mather, J. C., *Opt. Eng.*, 21, 769, 1982.
15. Gulkis, S., Lubin, P. M., Meyer, S. S., & Silverberg, R. F., *Sci. Amer.*, 262, 132, 1990.
16. Boggess, N. et al., *ApJ*, 397, 420, 1992.
17. Neugebauer, G. et al., *ApJ*, 278, L1, 1984.
18. Barney, R. D., *Illuminating Eng. Soc. J.*, 34, 34, 1991.
19. Milam, L. J., *Illuminating Eng. Soc. J.*, 34, 27, 1991.
20. Hopkins, R. A., & Castles, S. H., *Proc. SPIE*, 509, 207, 1985.
21. Hopkins, R. A., & Payne, D. A. *Adv. Cryogenic Engineering*, 33, 925, 1987.
22. Volz, S. M. & Ryschkewitsch, M. G., *Superfluid Helium Heat Transfer, HTD*, 134, 23, ed. J. P. Kelly & W. J. Schneider AME, New York, 1990.
23. Volz, S. M., Dipirro, M. J., Castles, S. H., Rhee, M. S., Ryschkewitsch, M. G., & Hopkins, R., *Proc. Internat. Symp. Optical and Opto-electronic Applied Sci. and Eng.*, 268, SPIE, San Diego, 1990.
24. Volz, S. M., Dipirro, M. J., Castles, S. H., Ryschkewitsch, M. G., & Hopkins, R., *Adv. Cryogenic Engineering*, 37A, 1183, 1991.
25. Volz, S. M. & DiPirro, M. J., *Cryogenics*, 32, 77, 1992.
26. Mosier, C. L. *AIAA*, 91-361, 1991.
27. Coladonato, R. J. et al., *Proc. Third Air Force/NASA Symp. on Recent Advances in Multidisciplinary Analysis and Optimization*, 370, Anamet, Hayward, CA, 1990.

28. Sampler, H. P. *Proc. SPIE*, 1340, 417, 1990.
29. Bromberg, B. W. & Croft, J. *Adv. Astron. Sci.*, 57, 217, 1985.
30. Smoot, G. F. et al., *ApJ*, 360, 685, 1990.
31. Bennett, C. L. et al., *ApJ*, 391, 466, 1992.
32. Torres, S., et al., *Data Analysis in Astronomy* eds. V. di gesu, L. Scarsi, & M. C. Maccarone, Erice, June 20-27, Plenum Press, 1989.
33. Smoot, G. F. et al., *ApJ*, 371, L1, 1991.
34. Smoot, G. F. et al., *ApJ*, 396, L1, 1992.
35. Kogut, A., et al., *ApJ*, in press, 1992.
36. Bennett, C. L. et al., *ApJ*, 396, L7, 1992.
37. Wright, E. L. et al., *ApJ*, 396, L13, 1992.
38. Fixsen, D. J., Cheng, E. S., & Wilkinson, D. T., *Phys.Rev.Lett.*, 50, 620, 1983.
39. Lubin, P., Villela, T., Epstein, G., & Smoot, G., *ApJ*, 298, L1, 1985.
40. Klypin, A. A., Sazhin, M. V., Strukov, I. A.,& Skulachev, D. P., *Sov.Astr.Letters*, 13, 104, 1987.
41. Meyer S. S., Page, L., & Cheng, E. S., *ApJ*, 371, L7, 1991.
42. Bertschinger, E., in *Current Topics in Astrofundamental Physics*, eds. N. Sanchez & Z. Zichini, in press and in *New Insights Into The Universe*, eds. V. J. Martinez, M. Portilla & D. Saez, in press, 1992.
43. Efstathiou, G., in *Physics of the Early Universe*, 361, eds. J. A. Peacock, A. F. Heavens, & A. T. Davies (Edinburgh Univ. Press: Edinburgh, Scotland), 1990.
44. Kolb, E., & Turner, M. S., *The Early Universe*, Addison Wesley, Redwood City, CA, 1987.
45. Peebles, P. J. E., *Physical Cosmology*, Princeton Univ. Press, Princeton, NJ, 1971.
46. Peebles, P. J. E., *The Large-Scale Structure of the Universe*, Princeton Univ. Press, Princeton, NJ, 1980.
47. Wilkinson, D. T., *Science*, 232, 1517, 1986.
48. Shafer, Fixsen, and Mather, 1993, this conference.
49. Fixsen, D. J. et al., submitted to *ApJ*, 1993.
50. Mather, J. C. et al., submitted to *ApJ*, 1993.
51. Wright, E. L. et al., submitted to *ApJ*, 1993.
52. Cheng, E. S. et al., *Bull.Am.Phys.Soc.*, 35, 971, 1990.
53. Fixsen, D. J. et al., submitted to *ApJ*, 1993.
54. Wright, E. L. et al., *ApJ*, 381, 200, 1991.
55. Petuchowski, S. J. & Bennett, C. L., *ApJ*, in press (1992)
56. Bond, J. R., Carr, B. J., & Hogan, C. J., *ApJ*, 306, 428, 1986.
57. Magner, T. J., *Opt.Eng.*, 26, 264, 1987.
58. Evans, D. C., *SPIE Proc.*, 384, 82, 1983.
59. Evans, D. C.& Breault, R. P., *SPIE Proc.*, 384, 90, 1983.
60. Hauser, M. G. et al.,*After the First Three Minutes*, 222, 161, eds. S. S. Holt, C. L. Bennett, & V. Trimble, AIP Conf. Proc, New York, 1991.
61. Hauser, M. G., *Back to the Galazy*, eds. S. S. Holt & F. Verter, AIP Conf. Proc, New York, to be published, 1993.
62. Berriman, G. B., et al. *Back to the Galazy*, eds. S. S. Holt & F. Verter, AIP Conf. Proc, New York, to be published, 1993.
63. Freudenreich, H. T., et al., *Back to the Galazy*, eds. S. S. Holt & F. Verter, AIP Conf. Proc, New York, to be published, 1993.
64. Arendt, R. G., et al., *Back to the Galazy*, eds. S. S. Holt & F. Verter, AIP Conf. Proc, New York, to be published, 1993.
65. Weiland, J. L., et al., *Back to the Galazy*, eds. S. S. Holt & F. Verter, AIP Conf. Proc, New York, to be published, 1993.
66. Sodroski, T. J., et al., *Back to the Galazy*, eds. S. S. Holt & F. Verter, (AIP Conf. Proc, New York, to be published, 1993.
67. Low, F. J. et al., *ApJ*, 278, L19, 1984.
68. White, R. A. & Mather, J. C., *Astrophysics and Space Sciences Library*, Vol.171, 29-34, ed. M. A. Albrecht & D. Egret Kluwer, Dordrecht, 1991.
69. Cheng, E. S. *Proc. 1st Annual Conf. on Astronomical Data Analysis Software and Systems*, NOAO, Tucson, AZ, in press, 1991.

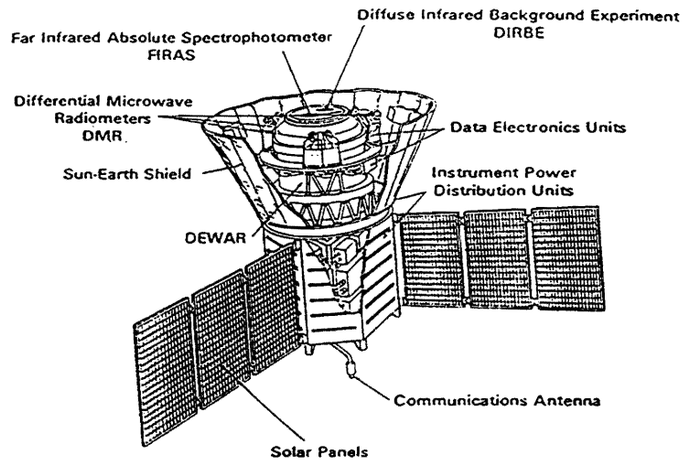

Figure 1: Artist cutaway drawing of the major components on COBE, showing the locations of the three scientific instruments.

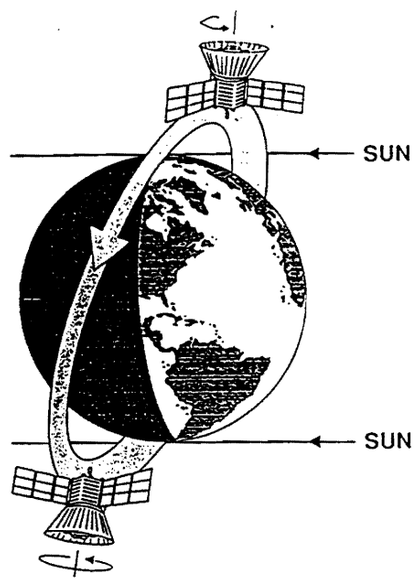

Figure 2: Schematic drawing of COBE in orbit. The orbit shows COBE in a high inclination orbit with its axis of rotation always pointing away from the Earth and about 90° from the Sun.

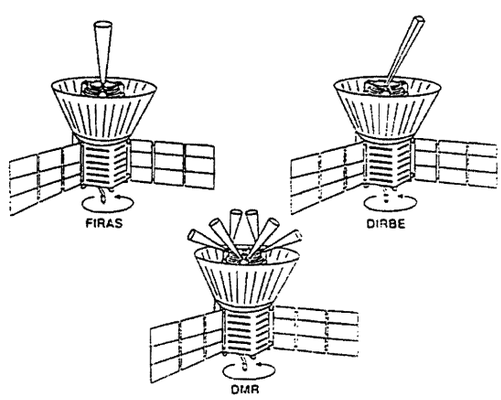

Figure 3: Schematic drawing of the viewing direction for each of the three instruments with respect to the spin axis of the spacecraft.